Plant Physiology and Biochemistry 170 (2022) 123–132

Contents lists available at ScienceDirect

Plant Physiology and Biochemistry

journal homepage: www.elsevier.com/locate/plaphy

Arabidopsis *N*-acetyltransferase activity 2 preferentially acetylates 1,3-diaminopropane and thialysine

Roberto Mattioli [a,1], Gianmarco Pascarella [b,1], Riccardo D'Incà [a], Alessandra Cona [a,d], Riccardo Angelini [a,d], Veronica Morea [c,**], Paraskevi Tavladoraki [a,d,*]

[a] Department of Science, University 'Roma Tre', Viale G. Marconi 446, Rome, 00146, Italy
[b] Department of Biochemical Sciences 'A. Rossi Fanelli', 'Sapienza' University, Rome, 00185, Italy
[c] Institute of Molecular Biology and Pathology, The National Research Council of Italy, Rome, 00185, Italy
[d] Interuniversity Consortium on Biostructures and Biosystems (INBB), Rome, 00136, Italy

ARTICLE INFO

Keywords:
AtNATA
1,3-Diaminopropane
N-acetyltransferases
Polyamines
Spermine
SSAT
Thialysine

ABSTRACT

Polyamine acetylation has an important regulatory role in polyamine metabolism. It is catalysed by GCN5-related *N*-acetyltransferases, which transfer acetyl groups from acetyl-coenzyme A to the primary amino groups of spermidine, spermine (Spm), or other polyamines and diamines, as was shown for the human Spermidine/Spermine N^1-acetyltransferase 1 (HsSSAT1). SSAT homologues specific for thialysine, a cysteine-derived lysine analogue, were also identified (*e.g.*, HsSSAT2). Two HsSSAT1 homologues are present in Arabidopsis, namely *N*-acetyltransferase activity (AtNATA) 1 and 2. AtNATA1 was previously shown to be specific for 1,3-diaminopropane, ornithine, putrescine and thialysine, rather than Spm and spermidine. In the present study, in an attempt to find a plant Spm-specific SSAT, *AtNATA2* was expressed in a heterologous bacterial system and catalytic properties of the recombinant protein were determined. Data indicate that recombinant AtNATA2 preferentially acetylates 1,3-diaminopropane and thialysine, throwing further light on AtNATA1 substrate specificity. Structural analyses evidenced that the preference of AtNATA1, AtNATA2 and HsSSAT2 for short amine substrates can be ascribed to different main-chain conformation or substitution of HsSSAT1 residues interacting with Spm distal regions. Moreover, gene expression studies evidenced that *AtNATA1* gene, but not *AtNATA2*, is up-regulated by cytokinins, thermospermine and Spm, suggesting the existence of a link between AtNATAs and N^1-acetyl-Spm metabolism. This study provides insights into polyamine metabolism and structural determinants of substrate specificity of non Spm-specific SSAT homologues.

1. Introduction

Polyamine acetylation has an important regulatory role in several organisms, since it affects both polyamine function and homeostasis (Pegg, 2008; Tavladoraki et al., 2012). Acetylation reduces the number of positive charges on polyamines, thus altering their capacity to interact with several macromolecules. In mammals, acetylated spermine (Spm) and spermidine (Spd) are substrates of peroxisomal polyamine oxidases (PAOs) and are readily secreted into the extracellular space, thus playing a key role in the control of intracellular polyamine levels and of cellular processes related to polyamine content (Pegg, 2008). In bacteria, polyamine acetylation neutralizes their toxicity and plays an important role in bacterial virulence and pathogenicity (Fukuchi et al., 1995; Barbagallo et al., 2011; Joshi et al., 2011; Planet et al., 2013). Acetylated polyamines have been also detected in several plant species, among which *Nicotiana plumbaginifolia*, *Helianthus tuberosus* and Arabidopsis (Del Duca et al., 1995; Mesnard et al., 2000; Tassoni et al., 2000; Fliniaux et al., 2004; Hennion et al., 2012; Toumi et al., 2019), but only

Abbreviations: Acetyl-coenzyme A, acetyl-CoA; CoA, coenzyme A; Dap, 1,3-diaminopropane; DTNB, 5,5-dithiobis-(2-nitrobenzoate); MSA, multiple sequence alignment; NATA, *N*-acetyltransferase activity; NHQ, N^1-Spm-acetyl-coenzyme A bi-substrate analogue; Nor-Spm, norspermine; PAO, polyamine oxidase; Orn, ornithine; Put, putrescine; SAT, Spd acetyltransferase; Spd, spermidine; Spm, spermine; SSAT, Spermidine/Spermine N^1-acetyltrasferase; T-Spm, thermospermine.

* Corresponding author. Department of Science, University 'Roma Tre', Viale G. Marconi 446, Rome, 00146, Italy.
** Corresponding author.
E-mail addresses: veronica.morea@cnr.it (V. Morea), paraskevi.tavladoraki@uniroma3.it (P. Tavladoraki).
[1] These authors have contributed equally to this work.

https://doi.org/10.1016/j.plaphy.2021.11.034
Received 27 July 2021; Received in revised form 18 November 2021; Accepted 20 November 2021
Available online 24 November 2021

limited information exists on their physiological roles. However, a role of acetylated polyamines in plant development and responses to environmental and biotic stress has been suggested (Tassoni et al., 2000; Hennion et al., 2006; Addio et al., 2011; Jammes et al., 2014; Lou et al., 2016).

Spermidine/Spermine N^1-acetyltransferases (SSATs) are GCN5-related *N*-acetyltransferases (Neuwald and Landsman, 1997) that catalyse the transfer of acetyl groups to the aminopropyl end(s) of Spd and Spm, using acetyl-coenzyme A (acetyl-CoA) as a cofactor. SSATs are present in several organisms, among which animals (Coleman et al., 1996; Montemayor and Hoffman, 2008; Lien et al., 2013), protozoan parasites (Rojas-Chaves et al., 1996) and bacteria (Zhang et al., 2012; Li et al., 2019). Human SSAT1 (HsSSAT1) is a highly regulated enzyme with broad substrate specificity, being able to acetylate substrates with the general structure $H_2N(CH_2)_3NHR$, including N^1-acetylSpm, sym-norspermine, and sym-norspermidine, but not putrescine (Put), N^1-acetylSpd, and sym-homospermidine, which have terminal aminobutyl groups (Della Ragione and Pegg, 1983; Hegde et al., 2007; Pegg, 2008). In contrast to HsSSAT1, *E. coli* Spd acetyltransferase (SAT), encoded by the *speG* gene, transfers the acetyl group from acetyl-CoA to either end of Spd (aminopropyl or aminobutyl end) (Fukuchi et al., 1994; Sugiyama et al., 2016). Interestingly, the acetyltransferase encoded by the human gene locus BC011751, annotated as HsSSAT2 (Coleman et al., 2004; Han et al., 2006) because of its sequence similarity with HsSSAT1, does not acetylate Spm or Spd, but rather thialysine, a structural analog of L-lysine, which is considered to be a source of metabolites with antioxidant properties and can act as an antimetabolite by competing with L-lysine (Jun et al., 2003; Coleman et al., 2004; Proietti et al., 2020). GCN5-related *N*-acetyltransferases that preferentially acetylate thialysine are also present in *Caenorhabditis elegans* (CeSSAT; Abo-Dalo et al., 2004), *Leishmania major* (LmSSAT; Lüersen et al., 2005) and *Schizosaccharomyces pombe* (SpSSAT; Coleman et al., 2004).

In Arabidopsis genome, two *SSAT*-like genes have been identified in adjacent positions: *AtNATA1* (*N-acetyltransferase activity 1*; At2g39030) and *AtNATA2* (At2g39020). *AtNATA1* is highly regulated (Adio et al., 2011; Jammes et al., 2014), differently from *AtNATA2* which is constitutively expressed (Adio et al., 2011; Lou et al., 2016). The *AtNATA1* gene was shown to encode for protein with *N*-acetyltransferase activity, though discrepancy exists among published data regarding AtNATA1 substrate specificity. Some data indicate that 1,3-diaminopropane (Dap) is the best substrate, followed by thialysine (Jammes et al., 2014), while other data indicate that ornithine (Orn) (Adio et al., 2011) or Put (Lou et al., 2016) are best substrates. Furthermore, it was suggested that AtNATA1, together with arginine decarboxylase 1, which was shown to have also N^{δ}-acetylOrn decarboxylase activity, provides a pathway for the synthesis of acetylated Put from N^{δ}-acetylOrn (Lou et al., 2020). Conversely, no information on AtNATA2 substrate specificity is available so far.

Acetylated polyamines are substrates of PAOs in plants as well. In particular, it was shown that the physiological substrates of the cytosolic AtPAO5, encoded by a gene up-regulated by cytokinins, Spm and thermospermine (T-Spm), are N^1-acetylSpm, Spm and T-Spm, and that the catalytic activity on N^1-acetylSpm is higher than on Spm (Ahou et al., 2014). It was also shown that AtPAO5 is involved in N^1-acetylSpm, Spm and T-Spm homeostasis and that it influences plant development and xylem differentiation through a T-Spm dependent mechanism (Alabdallah et al., 2017). However, the physiological role of AtPAO5 related to N^1-acetylSpm homeostasis has not been determined so far, partly because of the lack of information regarding N^1-acetylSpm biosynthetic pathway.

In the present study, to identify the physiological function of *AtNATA2*, and in particular to investigate whether AtNATA2 is a Spm-specific SSAT, the *AtNATA2* gene was expressed in a heterologous bacterial system and the catalytic properties of the recombinant protein were analysed. The results evidenced that, similarly to the close homolog AtNATA1, recombinant AtNATA2 is not Spm-specific. Instead, it preferentially acetylates Dap and thialysine, which are also the preferred substrates of AtNATA1 according to one of the previous reports (Jammes et al., 2014) and at variance with others (Adio et al., 2011; Lou et al., 2016). Thus, the N^1-acetyl-Spm biosynthetic pathway in plants is still to be unveiled. Structural analyses indicated that the preference of AtNATA2, AtNATA1 and HsSSAT2 for short polyamines can be ascribed to a different main-chain conformation and/or side-chain substitution of HsSSAT1 residues interacting with Spm distal regions with respect to the acetyl-CoA cofactor. In parallel, gene expression studies highlighted that *AtNATA1* gene, but not *AtNATA2*, is up-regulated by cytokinins, Spm and T-Spm, similarly to the *AtPAO5* gene.

2. Material and methods

2.1. Plant material, growth conditions and treatments

All experiments were performed with Arabidopsis (*Arabidopsis thaliana*) ecotype Columbia. For *in vitro* growth, seeds were sterilized, stratified and put on agar plates containing half-strength Murashige and Skoog basal medium with Gamborgs vitamins and 0.5% (w/v) sucrose (1/2MS). Seedlings were grown at 23 °C and under a 16/8 h light/dark photoperiod. For qRT-PCR analysis following hormone or polyamine treatment, 7-day-old seedlings grown on 1/2MS agar plates were transferred in 1/2MS liquid medium and were left to grow for seven more days. After addition of fresh medium, seedlings were treated with 5 μM 6-benzylaminopurine (BAP) for 6 h. Seedlings were also treated with various concentrations (*i.e.*, 0.1 mM, 0.5 mM and 1 mM) of Spm, T-Spm, Spd, Put or Dap for 24 h. Data obtained using the lowest polyamine concentration that significantly affected gene expression levels under our experimental conditions (*i.e.*, 0.5 mM) are reported.

2.2. Isolation and cloning of AtNATA2 cDNA

AtNATA2 cDNA was amplified through RT-PCR using the sequence-specific oligonucleotides *AtNATA2-F2/*(5′- GCCTCGCATATGGCAGC CGCCGCACCGCCACCGCCACC-3′)*/AtNATA2-R2* (5′- GGTACGCTC-GAGCTA*GTGGTGGTGGTGGTGGTGTCCTCC*GATGTTGACCTGAT-CAAAAGCTTCAAGAG-3′). The underlined regions in oligonucleotides *AtNATA2-F2* and *AtNATA2-R2* indicate *Nde*I and *Xho*I sites, respectively. The *AtNATA2-R2* primer was designed to insert the coding sequence of the dipeptide linker GlyGly followed by a 6-His-tag at the 3' terminus of *AtNATA2* cDNA and prior to the stop codon. The amplified cDNA was subcloned into the *pGEM-T Easy* vector (Promega), sequenced, and then cloned in the *pET17b* plasmid (Novagen) between *Nde*I and *Xho*I restriction sites (*AtNATA2-pET17b* construct). For heterologous expression of *AtNATA2* in *Escherichia coli*, *AtNATA2-pET17b* construct was introduced into BL21 (DE3) *E. coli* strain.

2.3. Heterologous expression of AtNATA2 in E. coli

To obtain recombinant AtNATA2, a culture of the BL21 (DE3) *E. coli* strain containing the *AtNATA2-pET17b* construct was treated with 0.4 mM isopropyl β-D-1-thiogalactopyranoside for 4 h at 30 °C. Following induction, the culture was centrifuged at 3,000 g, the bacterial pellet was resuspended in extraction buffer (100 mM Tris-HCl, 150 mM NaCl, 20% glycerol), and cells were disrupted by sonication. Cell lysate was tested by immunoblotting using an anti-$(His)_6$ antibody (Abcam) and enzyme activity assays to detect accumulation of recombinant protein.

2.4. Purification of recombinant AtNATA2 from E. coli

To purify AtNATA2 recombinant protein, bacterial cell lysates were applied to Ni^{2+}-charged Sepharose (GE Healthcare) equilibrated in extraction buffer. Resin was washed first with extraction buffer and then with 100 mM Tris-HCl, pH 7.8, 20 mM imidazole. Recombinant protein was eluted with 100 mM Tris-HCl, pH 7.8, 300 mM imidazole, and

dialyzed against 100 mM Tris-HCl, pH 7.8, 20% glycerol using centrifugal filter devices (Millipore) with a cut-off of 10 kDa.

2.5. Enzymatic activity assays

To determine the catalytic properties of recombinant AtNATA2, an *in vitro* assay was performed based on the quantification of CoA-SH released during reaction using the reagent 5,5-dithiobis-(2-nitrobenzoate) (DTNB; Bode et al., 1993; Coleman et al., 2004; Lin et al., 2010; Jammes et al., 2014), essentially as described by Jammes et al. (2014). In detail, reaction mixtures of 50 µl were prepared containing 100 mM Tris/HCl, pH 8.0, 1 mM acetyl-CoA, recombinant AtNATA2 (circa 0.3 µg) and 5 mM of various putative substrates (Dap, thialysine, Spm, Spd, Orn, Nor-Spm, Put and *N*-monoacetyl-Put. Conversely, *N*-monoacetyl-Dap could not be tested since it was not readily available. Following incubation at 30 °C for various time intervals, the reaction was stopped by adding 150 µl ethanol. To quantify the released CoA-SH, an aliquot of 500 µl of 0.2 mM DTNB in 100 mM Tris/HCl, pH 8.0 was added and absorption at 412 nm was measured. K_m values of recombinant AtNATA2 for various substrates were determined from Michaelis-Menten plots. Nonlinear least-squares fitting of data was performed using Graphpad Prism software. For stoichiometric analyses, 0.5 mM of Dap or Put were added to a reaction mixture containing recombinant AtNATA2 (circa 0.3 µg) and 2 mM acetyl-CoA. Released CoA-SH was quantified at various time points until the end of the reaction.

2.6. Quantitative RT-PCR analysis

Total RNA was isolated from whole Arabidopsis seedlings using the RNeasy Plant Mini kit (QIAGEN) or TRIzol® Reagent (Ambion). Residual genomic DNA in RNA samples was digested by the RNase-Free DNase Set (QIAGEN) according to the manufacturers' protocol. Synthesis of cDNA and PCR amplification were performed using GoTaq® 2-Step RT-qPCR System (Promega). The qPCR reactions were performed in a Corbett RG6000 (Corbett Life Science, QIAGEN) using the program: 95 °C for 2 min, followed by 40 cycles at 95 °C for 3 s and 60 °C for 30 s. The gene for ubiquitin-conjugating enzyme 21 (UBC21; At5g25760) was used as reference gene using the oligonucleotides *UBC21-for* (5-CTGCGACTCAGGGAATCTTCTAA-3′) and *UBC21-rev* (5-TTGTGCCATTGAATTGAACCC-3). For qRT–PCR analysis of *AtNATA1* and *AtNATA2* expression levels, the oligonucleotides *AtNATA1-qPCR-for* (5-GAGTCTGGTCTTGCCTCCAC-3), *AtNATA1-qPCR-rev* (5-ATGCGTCTCAAGAAAGGGG-3'), *AtNATA2-qPCR-for* (5-GCTTCTCTAGAACCTCTCCATCG-3) and *AtNATA2-qPCR-rev* (5-CATGTTTGGTTCCGGTGCTG-3) were used. Relative expression levels are expressed as fold-changes ($2^{-\Delta\Delta Ct}$). Reactions were performed in triplicate and mean values ± SE were calculated. At least three independent biological replicates were performed for each experiment, and mean values of relative expression levels from the different biological replicates are shown.

2.7. Sequence alignments and phylogenetic analysis

The sequences of proteins analysed in this work were downloaded from the UniProt knowledgebase (UniProt Consortium, 2019). Multiple sequence alignments were performed using Clustal Omega (ClustalO; https://www.ebi.ac.uk/Tools/msa/clustalo/; Sievers et al., 2011). Sequences were analysed for the presence of putative PEST motifs using the PESTFIND program (http://emboss.bioinformatics.nl/cgi-bin/emboss/epestfind; Rogers et al., 1986). The amino acid sequences of AtNATA1 (UniProt ID: Q9ZV05), AtNATA2 (UniProt ID: Q9ZV06), HsSSAT1 (UniProt ID: P21673) and HsSSAT2 (UniProt ID: Q96F10) were given as queries to the BLASTP program (Altschul et al., 1997) to identify homologous proteins by sequence similarity searches. Phylogenetic analyses of amino acid sequences were performed using the MEGA5 software (Stecher et al., 2020) and the Neighbour-Joining (NJ) method (bootstrap1000). Abbreviations and accession numbers are listed in Supplementary Table S1.

2.8. Homology modelling of AtNATA1 and AtNATA2 and structure analysis

The sequences of AtNATA1 and AtNATA2 were used to search the NCBI database for homologous proteins of known 3D structure using the BLASTp algorithm (https://blast.ncbi.nlm.nih.gov/Blast.cgi; Altschul et al., 1997). This search retrieved the proteins listed in Supplementary Table S2, the co-ordinate files of which were downloaded from the Protein Data Bank (PDB; http://www.rcsb.org/; Berman et al., 2000). Based on the E-values calculated by BLASTp, both AtNATA1 and AtNATA2 match most closely *Pseudomonas aeruginosa* probable *N*-acetyltransferase (E-values $1e^{-24}$ and $4e^{-21}$, respectively), then HsSSAT2 (E-values $3e^{-17}$ and $2e^{-15}$, respectively), followed by mouse SSAT1 (MmSSAT1; E-values $2e^{-16}$ and $3e^{-12}$, respectively) and HsSSAT1 (E-values $2e^{-15}$ and $4e^{-11}$, respectively). Considering that AtNATA1 and AtNATA2 E-values and percentage sequence identity with the bacterial enzyme were only marginally better than those with HsSSAT2 (Supplementary Table S3), HsSSAT2 was chosen as a template for AtNATA1 and AtNATA2 model building, because the alignments with both Arabidopsis proteins presented a lower number of inserted residues, and these were grouped in a smaller number of regions, which is the most commonly observed situation in protein evolution. Additionally, the structure determination of the *P. aeruginosa* protein is not associated with a peer-reviewed publication describing the details of the structure (Supplementary Table S2).

The 3D models of AtNATA1 and AtNATA2 were built using Swiss-Model (https://swissmodel.expasy.org/; Guex and Peitsch, 1997). The UCSF Chimera package (Pettersen et al., 2004) was used for 3D structure visualization, analysis and comparisons, including pairwise structure superimpositions. To model AtNATA1 and AtNATA2 complexes with acetyl-CoA and substrates, each 3D model was optimally superimposed to the HsSSAT1 structure and the co-ordinates of the CoA cofactor covalently bound to Spm were imported into each model. The Spm moiety was computationally modified to obtain Put, Orn and other ligands.

The structure-based multiple sequence alignment (MSA) shown in Fig. 1 was obtained as follows:

(i) ClustalO (https://www.ebi.ac.uk/Tools/msa/clustalo/; Sievers et al., 2011) was used to produce an initial MSA comprising AtNATA1, AtNATA2, their homologues of known structure listed in Supplementary Table S2, and additional homologues from other species, namely HsSSAT2-like from *Mus musculus* (MmSSAT2), and SSAT from *L. major* (LmSSAT), *C. elegans* (CeSSAT) and *S. pombe* (SpSSAT);

(ii) Structure superimpositions between each pair of structures present in the initial MSA were obtained as follows: An initial structure alignment was generated automatically by Chimera. A structural superimposition was then performed including only structurally aligned residues the Cα atoms of which were at a distance not higher than 2.2 Å. This procedure was repeated until all and only residue pairs satisfying this distance threshold were superimposed.

(iii) The initial MSA produced by ClustalO was thus manually adjusted based on the structure superposition between HsSSAT2, HsSSAT1 and the 3D models built for AtNATA1 and AtNATA2 (see below) to produce the structure-based MSA shown in Fig. 1. Of the two monomers present in the functional homodimer, HsSSAT2 chain B (comprising residues 2–59 and 70–170) was used in all comparisons, because it is more complete than chain A (comprising residues 3–30, 35–60 and 68–170). Chain B was also chosen as a reference for AtNATA2 and AtNATA1 models, since they were built using HsSSAT2 as a template. Chain A of HsSSAT1

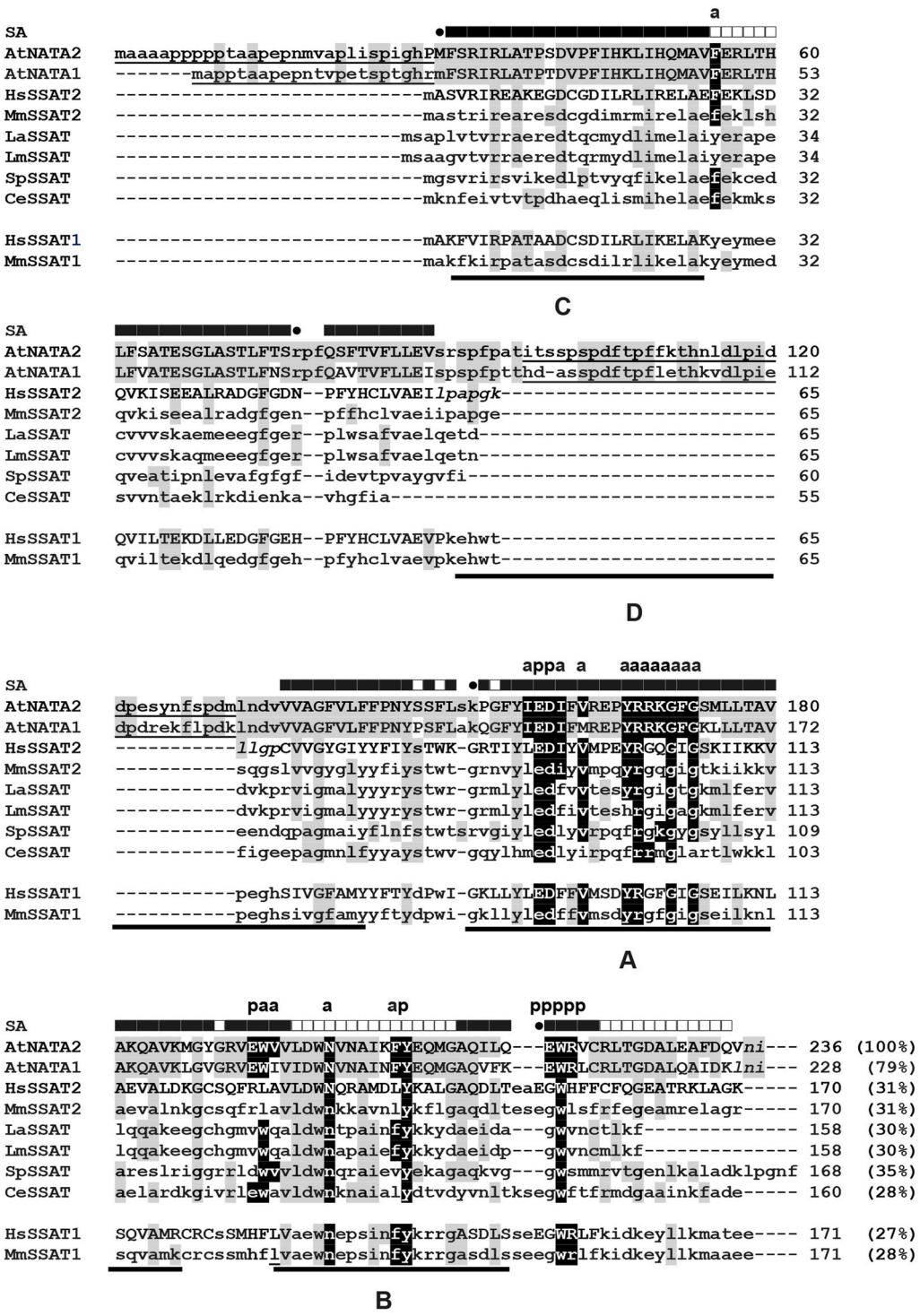

Fig. 1. Structure-based multiple sequence alignment comprising AtNATA1, AtNATA2 and homologous proteins from different species. Insertions and *N*-terminal extensions in AtNATA1 and AtNATA2 are underlined. "■", "□" and "●" symbols indicate the 115, 37 and 4 residues, respectively, which are structurally conserved in: i) AtNATA1 and AtNATA2 models, and HsSSAT2 and HsSSAT1 structures (HsSSAT2 residues: 3–26, 33–48, 50–59, 70–81, 83, 85, 87, 89–122, 124–129, 145–149, 153–157); ii) AtNATA1 and AtNATA2 models, and HsSSAT2 structure, but not HsSSAT1 (HsSSAT2 residues: 27–32, 82, 84, 88, 123, 130–144, 158–169); iii) HsSSAT2 and HsSSAT1 structures, but not AtNATA1 and AtNATA2 models (HsSSAT2 residues: 2, 49, 86, 152), respectively. Residues that are structurally aligned to each other are uppercase. Residues not observed in the 3D structure of HsSSAT2 chain B and residues that are not present in AtNATA1 or AtNATA2 models are shown in italic. Conserved structural domains in GCN5-related *N*-acetyltransferases (Neuwald and Landsman, 1997) are indicated by labelled horizontal bars (A, B, C, D). Positions involved in acetyl-CoA or polyamine binding are labelled with letters 'a' or 'p', respectively. Residues the identity of which is conserved with respect to AtNATA2, are black-shaded if they are found at positions labelled with 'a' or 'p' and grey-shaded otherwise. Numbers in parentheses indicate the percentage of amino acid sequence identity to AtNATA2. Sequence accession numbers are listed in Supplementary Table S1. At, *Arabidopsis thaliana*; Hs, *Homo sapiens*; Mm, *Mus musculus*; Lm, *Leishmania major*; Sp, *Schizosaccharomyces pombe*. Ce, *Caenorhabditis elegans*.

was selected because it provides the best structure superposition with HsSSAT2 chain B, whereas chain C of MmSSAT1 was chosen because it is the only one in complex with Spm. Throughout the text, residues belonging to the monomer chosen as reference are indicated by their three-letter code name and number along the sequence, and residues from the other monomer by the three-letter code, number and chain name. As an example, in HsSSAT1, Glu92 is from the reference monomer (chain A) and Trp154.B from the other one (chain B).

All software and databases used in this study are publicly available. For all software, default parameters and thresholds were used. Databases were last queried on December 12th, 2020. Images were generated using the UCSF Chimera package. Model co-ordinates are available from the authors upon request.

3. Results

3.1. Sequence analysis of Arabidopsis AtNATA1 and AtNATA2

AtNATA1 and *AtNATA2* genes, and their protein products, AtNATA1 and AtNATA2, are closely related to each other. In fact, they have

similar gene structure (being both intron-less), 76% nucleotide sequence identity and 79% amino acid sequence identity. AtNATA1 and AtNATA2 also have 31–32% identical amino acids with the thialysine-specific HsSSAT2 over 152 aligned residues and 27–28% identical amino acids with the Spm/Spd-specific HsSSAT1 over 119 aligned residues (Fig. 1). With respect to the human SSATs, AtNATA1 and AtNATA2 have an additional N-terminal region of 22 and 29 amino acids, respectively (Fig. 1). Moreover, these N-terminal regions are predicted to comprise a potential PEST motif (AtNATA1 with high probability, and AtNATA2 with low probability) and are found upstream of a methionine residue which is well aligned to the first methionine residue of HsSSAT1 and HsSSAT2, and thus may have a regulatory role at a post-transcriptional level (Supplementary Fig. S1). These N-terminal regions are highly conserved in most AtNATA homologues from dicots, but not in those from monocots, Amborella, Selaginella, Physcomitrella and the Solanales group II (Supplementary Fig. S1; Supplementary Fig. S2). AtNATA1 and AtNATA2 also present a long insertion (amino acid regions 45–105 and 75–135, respectively) with respect to homologous proteins of known structure (Fig. 1; Supplementary Fig. S1), which bears a putative PEST motive. BLASTp searches indicated that these insertions are only present in plant AtNATA-like sequences, and that neither of them is homologous to proteins of known structure.

The phylogenetic analysis of AtNATA homologues from representative plant species highlighted that the relationships among AtNATA-like amino acid sequences closely reflect the taxonomic evolutionary relationships between the plant families to which they belong. AtNATA1 and AtNATA2 are grouped together with AtNATA homologues of plants of the order of Brassicales. In this group, the two Arabidopsis proteins are found within distinct sub-groups, which indicates that *AtNATA1* and *AtNATA2* have evolved through a gene duplication event that occurred recently, during diversification of the Brassicales. However, the *AtNATA1* gene copy was lost in some of the Brassicales species, such as the Brassicaceae that have only the *AtNATA2* homolog (Lou et al., 2016). Similarly, AtNATA-like sequences from Malpighiales, Fabales, Cucurbitales and Poales form monophyletic groups. Only AtNATA-like sequences of Solanales form two distinct groups (Solanales I and II; Supplementary Fig. S2), due to a gene duplication event which took place after monocot and dicot divergence.

3.2. Substrate specificity of recombinant AtNATA2

AtNATA2 was expressed in *E. coli*, and the recombinant protein was purified by affinity chromatography to electrophoretic homogeneity (Supplementary Fig. S3). Catalytic properties of recombinant AtNATA2 were analysed by an *in vitro* assay based on the quantification of CoA-SH released during reaction (Bode et al., 1993; Coleman et al., 2004; Lin et al., 2010; Jammes et al., 2014). Recombinant AtNATA2 was shown to be more active towards Dap and thialysine than other substrates (Fig. 2; Table 1). Indeed, determination of catalytic constants indicated that the AtNATA2 catalytic efficiency (k_{cat}/K_m) towards Dap is similar to that measured with thialysine and 19- to 27-fold higher than that with Orn and Put (Table 1). AtNATA2 catalytic activity towards Dap was further shown to be higher at 30 °C than 23 °C, and at basic than acidic pH, reaching a maximum at pH 8.5 (Fig. 3). Furthermore, it was shown that AtNATA2 is able to exert catalytic activity towards *N*-monoacetyl-Put, though with a 7-fold lower k_{cat} value than towards Put (Table 1). In addition, stoichiometric analysis evidenced a molar ratio of around 2 between the released CoA-SH and consumed Dap or Put, indicating that Dap and Put are di-acetylated during the AtNATA2 catalysed reaction.

3.3. AtNATA1 and AtNATA2 structural analysis

To elucidate the structural determinants of substrate specificity, 3D models of AtNATA1 and AtNATA2 homodimers have been obtained (Fig. 4). Inspection of these models and of structure-based sequence alignments (Fig. 1) shows that the long insertions are located on the external sides of both proteins and are, therefore, not expected to affect the rest of the fold (Fig. 4). The core of the fold is predicted to be conserved with respect to HsSSAT2, to which both AtNATA1 and AtNATA2 monomers are aligned for 152 out of 170 total HsSSAT2 residues. Indeed, residues involved in acetyl-CoA binding are structurally conserved in AtNATA1 and AtNATA2 with respect to HsSSAT2, most of them being either identical or substituted by residues with similar physical-chemical properties (Fig. 1). However, differences in residue size are observed at a few positions, namely HsSSAT2 residues Gly102, Gln103, Ile105, Leu127 and Leu139, which in AtNATA1 and AtNATA2 are replaced by the bulkier Arg, Lys, Phe, Trp and Phe, respectively. With respect to HsSSAT1, AtNATA1 and AtNATA2 conserve the GCN5-related *N*-acetyltransferase fold in the A and C regions, but they are expected to diverge from HsSSAT1 in the B and D regions. Indeed, among HsSSAT1 residues involved in acetyl-CoA binding (Lu et al., 1996; Bewley et al., 2006; Zhu et al., 2006), residues Tyr100, Arg101, Gly104 and Gly106 are conserved in AtNATA1 and AtNATA2, and residues Tyr27 and Leu91 are conservatively substituted by Phe and Ile residues, respectively (Fig. 1). On the other hand, the short C terminal MATEE sequence, which was shown to be important in HsSSAT1 rapid *in vitro* degradation and for the stabilizing effect of polyamine analogues on HsSSAT1 (Coleman and Pegg, 1997), is not present in the two Arabidopsis proteins or in HsSSAT2 (Fig. 1).

Comparative analysis of the ligand binding pockets of AtNATA2 and AtNATA1 with those of HsSSAT2, HsSSAT1 and MmSSAT1 revealed that they present significant differences in shape, dimension and chemical-physical nature of surrounding residues (Fig. 1; Fig. 5; Fig. 6). These

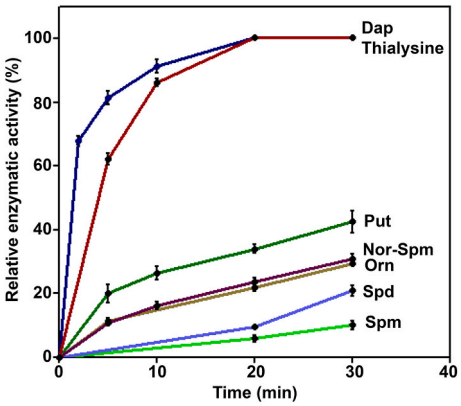

Fig. 2. Time course of acetyltransferase activity of recombinant AtNATA2 *in vitro* with different acetyl acceptors. Catalytic activity is reported as percentage relative to the maximum activity. Each point represents the mean value from three independent experiments and bars indicate SE. Dap: 1,3-diaminopropane; Nor-Spm: norspermine; Orn: ornithine; Put: putrescine; Spd: spermidine; Spm: spermine.

Table 1
Catalytic parameters of recombinant AtNATA2 with the indicated substrates. Values indicate means of three replicates ± SD. Acetyl-CoA: acetyl-coenzyme A; Dap: 1,3-diaminopropane; Nor-Spm: norspermine; Orn: ornithine; Put: putrescine; Spd: spermidine; Spm: spermine.

	k_{cat} (s^{-1})	K_m (mM)	k_{cat}/K_m ($mM^{-1}s^{-1}$)
Dap	1.02 ± 0.20	0.77 ± 0.18	1.33
Thialysine	0.78 ± 0.20	0.90 ± 0.36	0.87
Put	0.07 ± 0.023	1.29 ± 0.37	0.05
Orn	0.02 ± 0.005	0.29 ± 0.07	0.07
Nor-Spm	0.03 ± 0.010	2.73 ± 0.83	0.011
Spd	0.02 ± 0.004	1.70 ± 0.80	0.012
Spm	0.01 ± 0.006	n.d.*	n.d.
N-monoacetyl-Put	0.01 ± 0.005	n.d.	n.d.
Acetyl-CoA	n.d.	0.42 ± 0.06	n.d.

*n.d. = not determined.

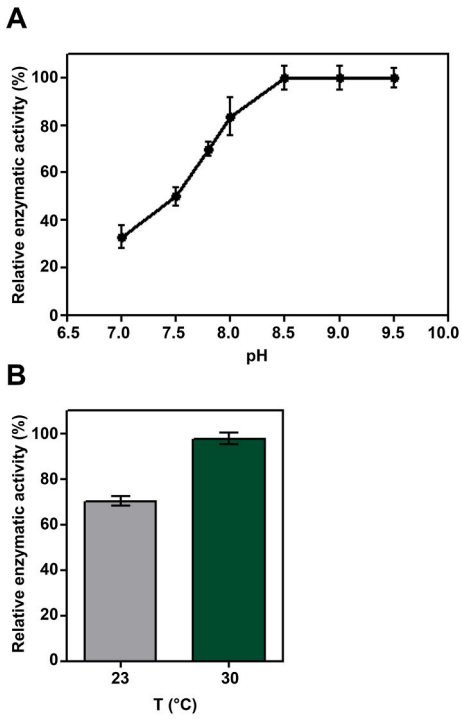

Fig. 3. Catalytic activity of recombinant AtNATA2 as a function of pH (A) and temperature (B). Catalytic activity was measured using Dap as a substrate. Data are expressed as percent of maximum activity. Each point represents the mean value from three independent experiments and bars indicate SE.

differences result from the fact that only a small fraction of HsSSAT1 acidic, hydrophobic and aromatic residues lining the Spm binding site are conserved in terms of both main-chain position and identity in AtNATA2, AtNATA1 and HsSSAT2 (Fig. 1; Fig. 5). These are: i) Asp93 and Glu92, which are within salt-bridge distance from the first (N^1) and second (N^2) Spm amino groups and participate in HsSSAT1 catalytic mechanism (Hegde et al., 2007; Bewley et al., 2006); and ii) Trp154 from the monomer not taken as reference (Trp154.B; see Materials and Methods), which makes hydrophobic contacts with the methylene groups between the second (N^2) and third (N^3) Spm amino group. Furthermore, Leu128 residue of HsSSAT1 catalytic site is conserved in main-chain position, but its side-chain is replaced by different aliphatic side-chains, such as those of Ile in AtNATA1 (Ile187), Val in AtNATA2 (Val195) and Ala in HsSSAT2 (Ala128). All of the other HsSSAT1 residues involved in interactions with Spm present significant differences in HsSSAT2 and the Arabidopsis homologues: i) HsSSAT1 Glu28, which interacts with the third (N^3) and fourth (N^4) Spm amino groups, is conserved in type in the other three enzymes (Glu28 in HsSSAT2, Glu49 in AtNATA1 and Glu56 in AtNATA2), but its main-chain and, consequently, side-chain is placed in a different position with respect to the other ligand-binding site residues; ii) Glu32, which interacts with Spm N^4, is replaced by His in AtNATA2 (His60) and AtNATA1 (His53), and conservatively substituted by Asp in HsSSAT2 (Asp32); iii) Asp82.B, which is salt-bridged to Spm N^3, is replaced by the hydrophobic Pro in AtNATA1 (Pro140.A) and by the polar Ser in AtNATA2 (Ser148.A) and HsSSAT2 (Ser82.A); iv) Trp84.B, which packs with the Spm methylene groups between N^3 and N^4, is conserved in HsSSAT2 (Trp84) and replaced by Phe in AtNATA2 (Phe150.A) and AtNATA1 (Phe142.A). As shown in Fig. 6, Trp84.B of HsSSAT1 packs with the methylene groups of Spm comprised between N^3 and N^4, whereas in HsSSAT2 3D structure the loop comprising Trp84.B assumes a different conformation that places the side-chain of HsSSAT2 in a position that would clash with Spm distal region. In the 3D models of AtNATA2 and AtNATA1, the homologous loops are predicted to assume a conformation similar to that of HsSSAT2, and the side-chains of Phe150.A and Phe142.A are predicted to assume a position similar to that of Trp84.A in HsSSAT2 and, therefore, overlap with the Spm region comprised between N^3 and N^4 as well (Fig. 6).

These data indicate that the preference of AtNATA2, AtNATA1 and HsSSAT2 for short substrates, comprising only two amino groups (such as Dap, Put and Orn), over substrates comprising three or four amino groups, is likely contributed by the fact that although HsSSAT1 residues interacting with Spm regions proximal to the acetyl-CoA cofactor (from $N^1$to N^2) are mostly conserved in both Arabidopsis protein and HsSSAT2, residues interacting with Spm distal regions (from N^3 to N^4) assume different conformation (like Glu28 and Trp84.B) and/or are replaced by residues differing in size (like Trp84.B), chemical nature (*e.*

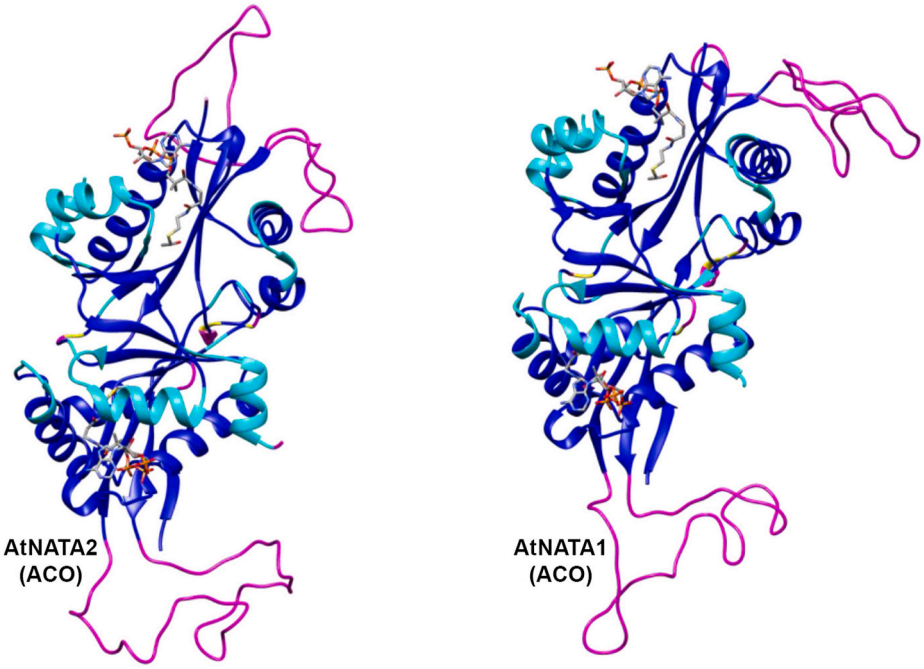

Fig. 4. 3D atomic models of AtNATA1 and AtNATA2 homodimers in complex with acetyl-CoA. In the models, main-chain atoms are represented as ribbon and colour-coded as follows: Blue, residues that are structurally conserved with respect to both HsSSAT2 and HsSSAT1 structures (indicated by "■" in Fig. 1); Cyan, residues that are structurally conserved with respect to HsSSAT2 structure, but not HsSSAT1 (indicated by "□" in Fig. 1); Yellow, residues that are structurally conserved between HsSSAT2 and HsSSAT1 structures, but not in AtNATA1 and AtNATA2 models (indicated by "●" in Fig. 1); Magenta, residues that are not structurally conserved in either of the aforementioned groups of structures. Acetyl-CoA (ACO) is shown as sticks and coloured by atom type (C, green; N, blue; O, red; P, orange).

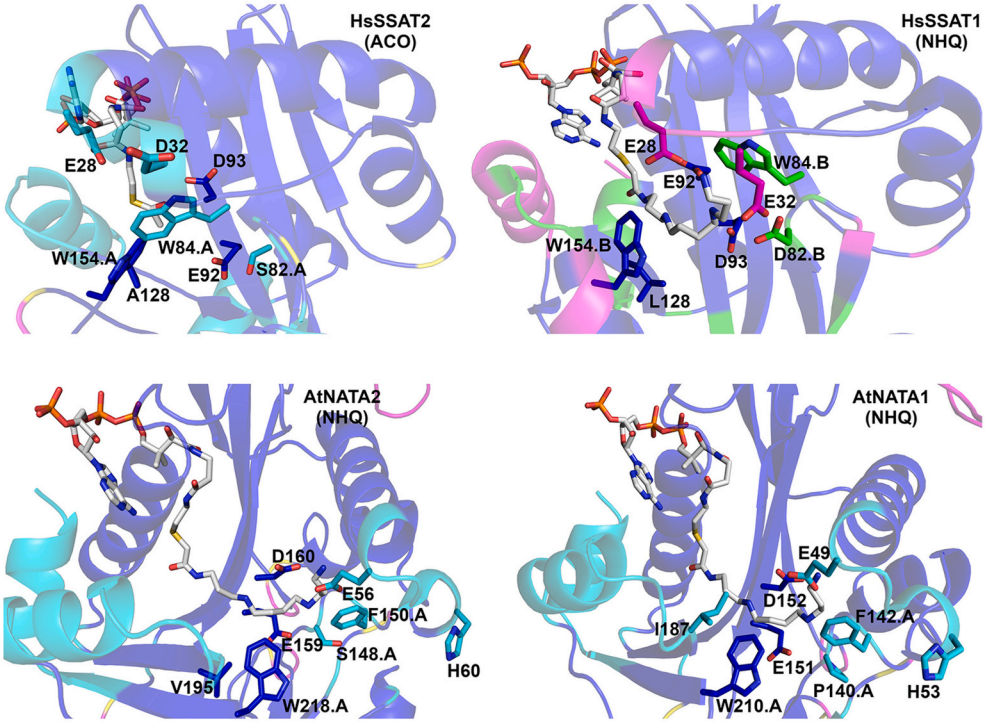

Fig. 5. Comparison among substrate binding-site residues of human SSAT structures and Arabidopsis NATA models. Ribbon representation of the 3D structures of HsSSAT2 and HsSSAT1 homodimers, which have been experimentally determined by X-ray crystallography (Han et al., 2006; Hegde et al., 2007), and of the atomic models of AtNATA2 and AtNATA1 homodimers, built in this work. Colour-coding is as follows: Blue, regions that are structurally conserved among HsSSAT2, HsSSAT1, AtNATA2 and AtNATA1 (indicated by "■" in Fig. 1); Cyan, regions that are structurally conserved among HsSSAT2, AtNATA2 and AtNATA1, but not HsSSAT1 (indicated by "□" in Fig. 1); Green, regions that are structurally conserved among HsSSAT1, AtNATA2 and AtNATA1, but not HsSSAT2; Magenta, other regions. Protein ligands, *i.e.*, acetyl-CoA (ACO; HsSSAT2) and N^1-Spm-acetyl-coenzyme A bi-substrate analogue (NHQ) comprising covalently linked acetyl-CoA and Spm (HsSSAT1, AtNATA2 and AtNATA2) are shown as sticks and coloured by atom type: N, O, C, S and P atoms are blue, red, white, yellow and orange, respectively. Residues interacting with Spm in HsSSAT1, and structurally equivalent residues in HsSSAT2, AtNATA2 and AtNATA1 are shown as sticks and coloured by atom type: N, O and S atoms are blue, red and yellow, respectively; C atoms are blue, cyan, green or magenta depending on the colouring of the ribbon.

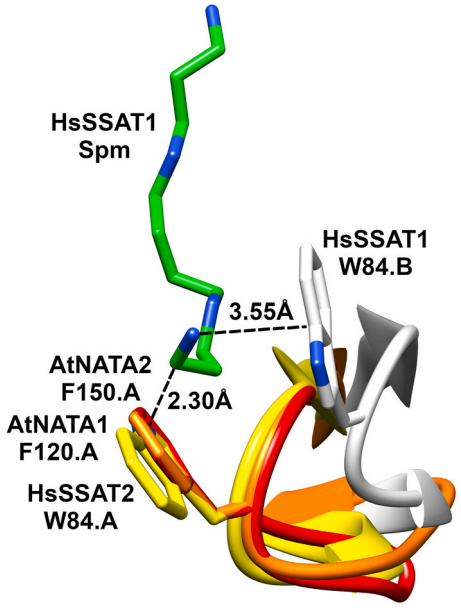

Fig. 6. Comparison among substrate binding-site pockets of human SSAT structures and Arabidopsis NATA models. The loop regions comprising residue Trp84.B of HsSSAT1 and HsSSAT2, Phe150.A of AtNATA2 and Phe142.A of AtNATA1 are shown as ribbon and coloured white, yellow, orange and red, respectively. The aforementioned residues and the Spm ligand of HsSSAT1 are shown as sticks and coloured by atom type (N, blue; O, red; C, white, yellow, orange, red and green in HsSSAT1, HsSSAT2, AtNATA2, AtNATA1 and Spm, respectively).

g., Glu32 replacement by His in AtNATA2 and AtNATA1) or both (Asp82.B replacement by Ser and Pro). Based on these observations, the lack of activity of HsSSAT1 towards short diamines, like Put and Dap, may be ascribed to the interaction of HsSSAT1 acidic residues, such as Glu28, Glu32 and Asp82.B, which are in contact with Spm N^3 or N^4 in the crystal structure, with one of the external amino groups of the diamines. This would result in the positioning of the other amino group in a location too distant from the acetyl-CoA cofactor for a reaction to occur.

3.4. Regulation of *AtNATA1* and *AtNATA2* gene expression

Studies on regulation of gene expression by qRT-PCR analyses evidenced that *AtNATA1* gene is highly regulated in agreement with previous studies (Adio et al., 2011; Jammes et al., 2014). Indeed, *AtNATA1* is up-regulated by BAP, as well as by the polyamines Spm and T-Spm (Fig. 7), but not Put, Dap and Spd. Differently from *AtNATA1*, *AtNATA2* expression levels remained unchanged under all the different conditions tested (Fig. 7).

4. Discussion

Dap is present in various organisms, such as bacteria and plants. Two pathways leading to Dap biosynthesis have been identified so far. In some bacteria species, such as *Acinetobacter baumannii* and *Vibrio cholerae*, Dap is produced following conversion of aspartate semialdehyde to L-2,4-diaminobutanoate by a 2-ketoglutarate 4-aminotransferase, and then conversion of L-2,4-diaminobutanoate to Dap by L-2,4-diaminobutanoate decarboxylase (Ikai and Yamamoto, 1994; Lee et al., 2009). In *P. aeruginosa* and plants, Dap is produced from polyamine catabolism by a spermidine dehydrogenase (Dasu et al., 2006) and a PAO with an *endo*-mode of substrate oxidation (Cona et al., 2006), respectively. However, plants may have an additional pathway for Dap

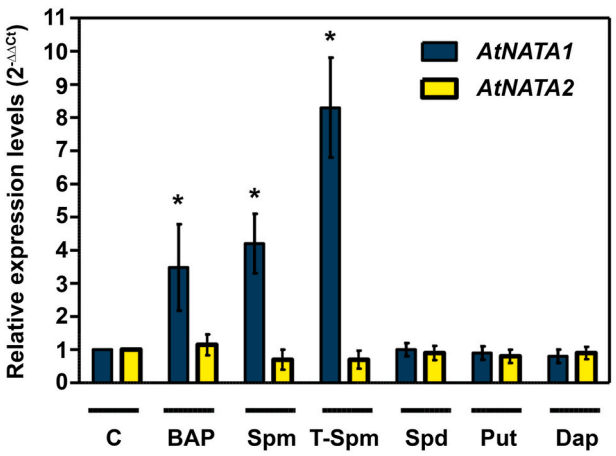

Fig. 7. Regulation of *AtNATA1* and *AtNATA2* gene expression by cytokinins and polyamines. Relative expression levels of *AtNATA1* and *AtNATA2* following treatment of 15-day-old Arabidopsis seedlings with 5 μM 6-benzylaminopurine (BAP) for 6 h and with 0.5 mM Spm, T-Spm, Spd, Put or Dap for 24 h. Expression levels were analysed by qRT-PCR. Mean values ± SE of relative expression levels from three independent replicates are shown. Asterisks denote statistically significant differences from the corresponding untreated seedlings (C; $P < 0.05$, one-way ANOVA).

biosynthesis, since not all plant species have a PAO with an *endo*-mode of substrate oxidation (Tavladoraki et al., 2016; Salvi and Tavladoraki, 2020). In plants, Dap may be a precursor of uncommon polyamines, which, in turn, are associated with stress tolerance (Cona et al., 2006). Furthermore, it has been suggested that in plants Dap is activated through acetylation to slow down abscisic acid-mediated stomata closure, probably as a homeostatic mechanism to maintain a proper balance between water loss and CO_2 uptake (Jammes et al., 2014).

In the present study, we investigated the catalytic properties of recombinant AtNATA2. The best polyamine substrate of the protein resulted to be Dap, whereas the catalytic efficiency towards Put, Spd and Spm and Orn is low. These data are consistent with data previously obtained for the closely related AtNATA1, which was reported to have high catalytic activity with Dap, and low with Spd and Spm (Jammes et al., 2014). However, differently from AtNATA1, which has 2.5-fold lower activity with thialysine (a metabolite which has not been detected in plants yet) than with Dap, recombinant AtNATA2 has high catalytic activity with thialysine as well (65% of the catalytic activity towards Dap). This difference between AtNATA1 and AtNATA2 suggests that small differences in the amino acid sequence of SSATs can influence substrate specificity. This was also observed for HsSSAT1 and HsSSAT2 that, despite high sequence identity (46%), exhibit different substrate specificity, HsSSAT1 being Spm- and Spd-specific, and HsSSAT2 thialysine-specific (Coleman et al., 2004). Data presented herein appear to be in contrast with previous data showing that recombinant AtNATA1 is mainly active with Put and Orn, the acetylated forms of which have been associated with defense responses (Adio et al., 2011; Lou et al., 2016). These contradictory data regarding recombinant AtNATA1 and AtNATA2 proteins may be reconciled by the possibility that the native enzymes acetylate all three metabolites under conditions in which intracellular Put or Orn levels exceed Dap levels, as was shown for Arabidopsis plants (Sánchez-López et al., 2009). Anyhow, all studies show that AtNATA1 and AtNATA2 have low activity with Spm and Spd. Therefore, the enzymes involved in N^1-acetyl-Spd and N^1-acetyl-Spm biosynthesis in Arabidopsis have still to be identified.

The k_{cat} and K_m values obtained for AtNATA2 using Dap as a substrate (1.02 s^{-1} and 0.77 mM, respectively) show that this enzyme has a catalytic efficiency (1.33×10^3 $M^{-1}s^{-1}$), which is 3- to 1000-fold lower than that of the other SSATs characterized so far. Indeed, HsSSAT1 k_{cat} towards Spd is 8.7 s^{-1} (Coleman et al., 2004) and the k_{cat} values of HsSSAT2, SpSSAT, CeSSAT and LmSSAT towards their best substrate (thialysine) are in the range 5.25–46 s^{-1} (Abo-Dalo et al., 2004; Coleman et al., 2004; Lüersen et al., 2005). Additionally, the K_m values and catalytic efficiencies of HsSSAT1, HsSSAT2, SpSSAT, CeSSAT and LmSSAT towards their best substrates are in the range 0.003–1.96 mM and 3.6×10^3 - 1.35×10^6 M^{-1} s^{-1}, respectively (Abo-Dalo et al., 2004; Coleman et al., 2004; Lüersen et al., 2005). These differences between AtNATA2 and the other so far characterised SSATs suggest that Dap and/or thialysine may not be the physiological substrates of AtNATA2. Furthermore, recombinant AtNATA2 expressed in a prokaryotic heterologous system may present some local structural differences with respect to the native conformation of the plant produced protein.

It has been previously shown that AtPAO5 catalyses the oxidation of Spm, T-Spm and N^1-acetyl-Spm and is involved in the homeostasis of these polyamines (Ahou et al., 2014; Alabdallah et al., 2017). Furthermore, *AtPAO5* is up-regulated by cytokinins, Spm and T-Spm and interferes with auxin and cytokinin signaling pathways, thus contributing to plant growth and xylem differentiation (Alabdallah et al., 2017). Interestingly, although neither AtNATA1 nor AtNATA2 are specific for Spm and Spd, *AtNATA1*, but not *AtNATA2*, was shown to be up-regulated by cytokinins, Spm and T-Spm similarly to *AtPAO5*. This suggests the existence of a link between AtNATA1 and AtPAO5, which is still to be elucidated.

Previews structural and biochemical studies suggested that HsSSAT1 and MmSSAT1 catalyse the acetyl transfer reaction through an acid/base-based catalytic mechanism, during which a catalytic base deprotonates the N^1-amine of the polyamine and a catalytic acid protonates the sulphur of acetyl-CoA (Hegde et al., 2007; Montemayor and Hoffman, 2008). Indeed, Tyr140 and Glu92 residues are positioned well inside the catalytic site to fulfil the role of a catalytic acid and base, respectively (Hegde et al., 2007; Montemayor and Hoffman, 2008). The present structural studies showed that these amino acids are conserved in AtNATA1 and AtNATA2 suggesting that the general catalytic mechanism is conserved in these plant enzymes. The present structural analyses also suggest that the preference of AtNATA1, AtNATA2 and HsSSAT2 for short amines can be attributed to their ligand binding pockets which differ in shape and chemical-physical nature from those of HsSSAT1 and MmSSAT1.

Overall, this study gives an insight into polyamine acetylation in plants and contributes to understanding polyamine metabolism and physiological roles. Moreover, it provides a comparison among the structural determinants of substrate specificity of different plant and human SSAT homologues.

Contributions

PT conceived the research plan. RM, RD and PT performed the experiments. PT made the phylogenetic analyses. GP and VM performed the structural analyses. PT and VM wrote the manuscript. AC and RA provided advice and comments for the manuscript.

Declaration of competing interest

The authors declare that they have no known competing financial interests or personal relationships that could have appeared to influence the work reported in this paper.

Acknowledgements

We wish to thank Prof. Andrea Bellelli (Department of Biochemical Sciences 'A. Rossi Fanelli', Sapienza University of Rome, Italy) for useful suggestions. This work was supported by the University 'Roma Tre' and the Italian Ministry of Education, University and Research: grant to the Department of Science of University 'Roma Tre' ('Dipartimenti di Eccellenza', ARTICOLO 1, COMMI 314-337. LEGGE 423 232/2016), grant to R.A. (PRIN 2017, CUP F84I19000730005) and grant to V.M.

(PRIN 2017, project 2017483NH8_005).

Appendix A. Supplementary data

Supplementary data to this article can be found online at https://doi.org/10.1016/j.plaphy.2021.11.034.

References

Abo-Dalo, B., Ndjonka, D., Pinnen, F., Liebau, E., Luersen, K., 2004. A novel member of the GCN5-related N-acetyltransferase superfamily from *Caenorhabditis elegans* preferentially catalyses the N-acetylation of thialysine [*S*-(2-aminoethyl)-L-cysteine]. Biochem. J. 383, 129–137.

Adio, A.M., Clare, L., Casteel, C.L., De Vos, M., Kim, J.H., Joshi, V., Li, B., Juéry, C., Daron, J., Kliebenstein, D.J., Jander, G., 2011. Biosynthesis and defensive function of N^{δ}-acetylornithine, a jasmonate-induced Arabidopsis metabolite. Plant Cell 23, 3303–3318.

Ahou, A., Martignago, D., Alabdallah, O., Tavazza, R., Stano, P., Macone, A., Pivato, M., Masi, A., Rambla, J.L., Vera-Sirera, F., Angelini, R., Federico, R., Tavladoraki, P., 2014. A plant spermine oxidase/dehydrogenase regulated by the proteasome and polyamines. J. Exp. Bot. 65, 1585–1603.

Alabdallah, O., Ahou, A., Mancuso, N., Pompili, V., Macone, A., Pashkoulov, D., Stano, P., Cona, A., Angelini, R., Tavladoraki, P., 2017. The Arabidopsis polyamine oxidase/dehydrogenase 5 interferes with cytokinin and auxin signaling pathways to control xylem differentiation. J. Exp. Bot. 68, 997–1012.

Altschul, S.F., Madden, T.L., Schäffer, A.A., Zhang, J., Zhang, Z., Miller, W., Lipman, D.J., 1997. Gapped BLAST and PSI-BLAST: a new generation of protein database search programs. Nucleic Acids Res. 25, 3389–3402.

Barbagallo, M., Di Martino, M.L., Marcocci, L., Pietrangeli, P., De Carolis, E., Casalino, M., Colonna, B., Prosseda, G., 2011. A new piece of the Shigella pathogenicity puzzle: spermidine accumulation by silencing of the speG gene. PLoS One 6, e27226.

Berman, H.M., Westbrook, J., Feng, Z., Gilliland, G., Bhat, T.N., Weissig, H., Shindyalov, I.N., Bourne, P.E., 2000. The protein Data Bank. Nucleic Acids Res. 28, 235–242.

Bewley, M.C., Graziano, V., Jiang, J., Matz, E., Studier, F.W., Pegg, A.E., Coleman, C.S., Flanagan, J.M., 2006. Structures of wild-type and mutant human spermidine/spermine N^1-acetyltransferase, a potential therapeutic drug target. Proc. Natl. Acad. Sci. U.S.A. 103, 2063–2068.

Bode, R., Thurau, A.M., Schmidt, H., 1993. Characterization of acetyl-CoA:L-lysine N6-acetyltransferase, which catalyzes the first step of carbon catabolism from lysine in *Saccharomyces cerevisiae*. Arch. Microbiol. 160, 397–400.

Coleman, C.S., Pegg, A.E., 1997. Proteasomal degradation of spermidine/spermine N1-acetyltransferase requires the carboxyl-terminal glutamic acid residues. J. Biol. Chem. 272, 12164–12169.

Coleman, C.S., Huang, H., Pegg, A.E., 1996. Structure and critical residues at the active site of spermidine/spermine N1-acetyltransferase. Biochem. J. 316, 697–701.

Coleman, C.S., Stanley, A.B., Jones, D.A., Pegg, A.E., 2004. Spermidine/spermine-N^1-acetyltransferase2 (SSAT) acetylates thialysine and is not involved in polyamine metabolism. Biochem. J. 384, 139–148.

Cona, A., Rea, G., Angelini, R., Federico, R., Tavladoraki, P., 2006. Functions of amine oxidases in plant development and defence. Trends Plant Sci. 11, 80–88.

Consortium, UniProt, 2019. UniProt: a worldwide hub of protein knowledge. Nucleic Acids Res. 47, D506–D515.

Dasu, V.V., Nakada, Y., Ohnishi-Kameyama, M., Kimura, K., Itoh, Y., 2006. Characterization and a role of *Pseudomonas aeruginosa* spermidine dehydrogenase in polyamine catabolism. Microbiology 152, 2265–2272.

Del Duca, S., Beninati, S., Serafini-Fracassini, D., 1995. Polyamines in chloroplasts: identification of their glutamyl and acetyl derivatives. Biochem. J. 305, 233–237.

Della Ragione, F., Pegg, A.E., 1983. Studies of the specificity and kinetics of rat liver spermidine/spermine N1-acetyltransferase. Biochem. J. 213, 701–706.

Fliniaux, O., Mesnard, F., Raynaud-Le Grandic, S., Baltora-Rosset, S., Bienaimé, C., Robins, R.J., Fliniaux, M.A., 2004. Altered nitrogen metabolism associated with de-differentiated suspension cultures derived from root cultures of *Datura stramonium* studied by heteronuclear multiple bond coherence (HMBC) NMR spectroscopy. J. Exp. Bot. 55, 1053–1060.

Fukuchi, J., Kashiwagi, K., Takio, K., Igarashi, K., 1994. Properties and structure of spermidine acetyltransferase in *Escherichia coli*. J. Biol. Chem. 269, 22581–22585.

Fukuchi, J., Kashiwagi, K., Yamagishi, M., Ishihama, A., Igarashi, K., 1995. Decrease in cell viability due to the accumulation of spermidine in spermidine acetyltransferase-deficient mutant of *Escherichia coli*. J. Biol. Chem. 270, 18831–18835.

Guex, N., Peitsch, M.C., 1997. SWISS-MODEL and the Swiss-PdbViewer: an environment for comparative protein modeling. Electrophoresis 18, 2714–2723.

Han, B.W., Bingman, C.A., Wesenberg, G.E., Phillips, G.N., 2006. Crystal structure of *Homo sapiens* thialysine N^{ϵ}-acetyltransferase (HsSSAT2) in complex with acetyl coenzyme A. Proteins 64, 288–293.

Hegde, S.S., Chandler, J., Vetting, M.W., Yu, M., Blanchard, J.S., 2007. Mechanistic and structural analysis of human spermidine/spermine N^1-acetyltransferase. Biochemistry 46, 7187–7195.

Hennion, F., Frenot, Y., Martin-Tanguy, J., 2006. High flexibility in growth and polyamine composition of the crucifer *Pringlea antiscorbutica* in relation to environmental conditions. Physiol. Plantarum 127, 212–224.

Hennion, F., Bouchereau, A., Gauthier, C., Hermant, M., Vernon, P., Prinzing, A., 2012. Variation in amine composition in plant species: how it integrates macro evolutionary and environmental signals. Am. J. Bot. 99, 36–45.

Ikai, H., Yamamoto, S., 1994. Cloning and expression in *Escherichia coli* of the gene encoding a novel L-2,4-diaminobutyrate decarboxylase of *Acinetobacter baumannii*. FEMS Microbiol. Lett. 124, 225–228.

Jammes, F., Leonhardt, N., Tran, D., Bousserouel, H., Véry, A.A., Renou, J.P., Vavasseur, A., Kwak, J.M., Sentenac, H., Bouteau, F., Leung, J., 2014. Acetylated 1,3-diaminopropane antagonizes abscisic acid-mediated stomatal closing in Arabidopsis. Plant J. 79, 322–333.

Joshi, G.S., Spontak, J.S., Klapper, D.G., Richardson, A.R., 2011. Arginine catabolic mobile element encoded speG abrogates the unique hypersensitivity of *Staphylococcus aureus* to exogenous polyamines. Mol. Microbiol. 82, 9–20.

Jun, D.Y., Rue, S.W., Han, K.H., Taub, D., Lee, Y.S., Bae, Y.S., Kim, Y.H., 2003. Mechanism underlying cytotoxicity of thialysine, lysine analog, toward human acute leukemia Jurkat T cells. Biochem. Pharmacol. 66, 2291–2300.

Lee, J., Sperandio, V., Frantz, D.E., Longgood, J., Camilli, A., Phillips, M.A., Michael, A. J., 2009. An alternative polyamine biosynthetic pathway is widespread in bacteria and essential for biofilm formation in *Vibrio cholerae*. J. Biol. Chem. 284, 9899–9907.

Li, B., Maezato, Y., Kim, S.H., Kurihara, S., Liang, J., Michael, A.J., 2019. Polyamine-independent growth and biofilm formation, and functional spermidine/spermine N-acetyltransferases in *Staphylococcus aureus* and *Enterococcus faecalis*. Mol. Microbiol. 111, 159–175.

Lien, Y.C., Ou, T.Y., Lin, Y.T., Kuo, P.C., Lin, H.J., 2013. Duplication and diversification of the spermidine/spermine N1-acetyltransferase 1 genes in zebrafish. PLoS One 8, e54017.

Lin, H.J., Lien, Y.C., Hsu, C.H., 2010. A high-throughput colorimetric assay to characterize the enzyme kinetic and cellular activity of spermidine/spermine N^1-acetyltransferase 1. Anal. Biochem. 407, 226–232.

Lou, Y.R., Bor, M., Yan, J., Preuss, A.S., Jander, G., 2016. Arabidopsis NATA1 acetylates putrescine and decreases defense-related hydrogen peroxide accumulation. Plant Physiol 171, 1443–1455.

Lou, Y.R., Ahmed, S., Yan, J., Adio, A.M., Powell, H.M., Morris, P.F., Jander, G., 2020. *Arabidopsis* ADC1 functions as an N^{δ}-acetylornithine decarboxylase. J. Integr. Plant Biol. 62, 601–613.

Lu, L., Berkey, K.A., Casero, R.A., 1996. RGFGIGS is an amino acid sequence required for acetyl coenzyme A binding and activity of human spermidine/spermine N^1-acetyltransferase. J. Biol. Chem. 271, 18920–18924.

Lüersen, K., 2005. *Leishmania major* thialysine N^{ϵ}-acetyltransferase: identification of amino acid residues crucial for substrate binding. FEBS (Fed. Eur. Biochem. Soc.) Lett. 579, 5347–5352.

Mesnard, F., Azaroual, N., Marty, D., Fliniaux, M.A., Robins, R.J., Vermeersch, G., Monti, J.P., 2000. Use of 15N reverse gradient two-dimensional nuclear magnetic resonance spectroscopy to follow metabolic activity in *Nicotiana plumbaginifolia* cell-suspension cultures. Planta 210, 446–453.

Montemayor, E.J., Hoffman, D.W., 2008. The crystal structure of spermidine/spermine N1-acetyltransferase in complex with spermine provides insights into substrate binding and catalysis. Biochemistry 47, 9145–9153.

Neuwald, A.F., Landsman, D., 1997. GCN5-related histone N-acetyltransferases belong to a diverse superfamily that includes the yeast SPT10 protein. Trends Biochem. Sci. 22, 154–155.

Pegg, A.E., 2008. Spermidine/spermine-N(1)-acetyltransferase: a key metabolic regulator. Am. J. Physiol. Endocrinol. Metab. 294, 995–1010.

Pettersen, E.F., Goddard, T.D., Huang, C.C., Couch, G.S., Greenblatt, D.M., Meng, E.C., Ferrin, T.E., 2004. UCSF Chimera-a visualization system for exploratory research and analysis. J. Comput. Chem. 25, 1605–1612.

Planet, P.J., LaRussa, S.J., Dana, A., Smith, H., Xu, A., Ryan, C., et al., 2013. Emergence of the epidemic methicillin-resistant *Staphylococcus aureus* strain USA300 coincides with horizontal transfer of the arginine catabolic mobile element and speG-mediated adaptations for survival on skin. mBio 4, e00889, 00813.

Proietti, G., Rainone, G., Hintzen, J.C.J., Mecinović, J., 2020. Exploring the histone acylome through incorporation of gamma-thialysine on histone tails. Bioconjugate Chem. 31, 844–851.

Rogers, S.W., Wells, R., Rechsteiner, M., 1986. Amino acid sequences common to rapidly degraded proteins: the PEST hypothesis. Science 234, 364–368.

Rojas-Chaves, M., Hellmund, C., Walter, R.D., 1996. Polyamine N-acetyltransferase in *Leishmania amazonensis*. Parasitol. Res. 82, 435–438.

Salvi, D., Tavladoraki, P., 2020. The tree of life of polyamine oxidases. Sci. Rep. 10, 17858.

Sánchez-López, J., Camanes, G., Flors, V., Vicent, C., Pastor, V., Vicedo, B., Cerezo, M., Garcia-Agustin, P., 2009. Underivatized polyamine analysis in plant samples by ion pair LC coupled with electrospray tandem mass spectrometry. Plant Physiol. Biochem. 47, 592–598.

Sievers, F., Wilm, A., Dineen, D., Gibson, T.J., Karplus, K., Li, W., Lopez, R., McWilliam, H., Remmert, M., Söding, J., Thompson, J.D., Higgins, D.G., 2011. Fast, scalable generation of high-quality protein multiple sequence alignments using Clustal Omega. Mol. Syst. Biol. 7, 539.

Stecher, G., Tamura, K., Kumar, S., 2020. Molecular evolutionary genetics analysis (MEGA) for macOS. Mol. Biol. Evol. 37, 1237–1239.

Sugiyama, S., Ishikawa, S., Tomitori, H., Niiyama, M., Hirose, M., Miyazaki, Y., Higashi, K., Murata, M., Adachi, H., Takano, K., Murakami, S., Inoue, T., Mori, Y., Kashiwagi, K., Igarashi, K., Matsumura, H., 2016. Molecular mechanism underlying promiscuous polyamine recognition by spermidine acetyltransferase. Int. J. Biochem. Cell Biol. 76, 87–97.

Tassoni, A., van-Buuren, M., Franceschetti, M., Fornale, S., Bagni, N., 2000. Polyamine content and metabolism in Arabidopsis thaliana and effect of spermidine on plant development. Plant Physiol. Biochem. 38, 383–393.
Tavladoraki, P., Cona, A., Federico, R., Tempera, G., Viceconte, N., Saccoccio, S., Battaglia, V., Toninello, A., Agostinelli, E., 2012. Polyamine catabolism: target for antiproliferative therapies in animals and stress tolerance strategies in plants. Amino Acids 42, 411–426.
Tavladoraki, P., Cona, A., Angelini, R., 2016. Copper-containing amine oxidases and FAD-dependent polyamine oxidases are key players in plant tissue differentiation and organ development. Front. Plant Sci. 7, 824.
Toumi, I., Pagoulatou, M.G., Margaritopoulou, T., Milioni, D., Roubelakis-Angelakis, K. A., 2019. Genetically modified heat shock protein90s and polyamine oxidases in Arabidopsis reveal their interaction under heat stress affecting polyamine acetylation, oxidation and homeostasis of reactive oxygen species. Plants 8, 323.
Zhang, Y., Zhou, J., Chang, M., Bai, L., Shan, J., Yao, C., Jiang, R., Guo, L., Zhang, R., Wu, J., Li, Y., 2012. Characterization of and functional evidence for Ste27 of Streptomyces sp. 139 as a novel spermine/spermidine acetyltransferase. Biochem. J. 443, 727–734.
Zhu, Y.-Q., Zhu, D.-Y., Yin, L., Zhang, Y., Vonrhein, C., Wang, D.-C., 2006. Crystal structure of human spermidine/spermine N1-acetyltransferase (hSSAT): the first structure of a new sequence family of transferase homologous superfamily. Proteins 63, 1127–1131.